Effects of Molecular Structure on Segment Orientation in Poly(diethylsiloxane) Elastomers. 2. NMR Measurements from Uniaxially Stretched Samples

Ronald C. Hedden, Hiroyasu Tachibana, T. M. Duncan, and Claude Cohen*

Olin Hall, School of Chemical Engineering, Cornell University, Ithaca, New York 14853

Received March 6, 2001; Revised Manuscript Received May 31, 2001

ABSTRACT: End-linked poly(diethylsiloxane) networks containing $-CD_2CH_3$ groups were studied in uniaxial extension by solid-state ^2H NMR. Chain segment orientation was measured for samples at low extension ratios in the amorphous state. At higher extension ratios, a localized phase transition to a mesomorphic "neck" can occur. The mesophase content and segment orientation in the neck region were probed by NMR at various extension ratios. The effects of chemical cross-link density on segment orientation were deduced by studying a series of samples with varying molecular weight between cross-links.

Introduction

Networks of poly(diethylsiloxane), PDES, can undergo an intriguing strain-induced phase transition to an aligned mesomorphic state. An initially amorphous PDES network placed under sufficient uniaxial tension can spontaneously develop a "neck" region with a mesomorphic structure.[1−5] This discrete localized transition is fundamentally different from strain-induced crystallization in other polymers such as natural rubber. In conventional crystallizable elastomers, a uniform dispersion of crystallites develops throughout the material as it is strained. On the contrary, the formation of the neck in PDES is a spontaneous shape change that has a marked influence on the mechanical and optical properties of the elastomer.

Formation of an oriented mesophase is typically exhibited by the chemically complex nematic liquid-crystalline polymer melts and networks[6−10] but is unusual for a pure homopolymer with no rigid "mesogens". The existence of a mesophase in PDES melts of molecular weight higher than 28 000 g/mol[11] and the amorphous-to-mesophase transition of amorphous PDES networks subjected to uniaxial extension occur at the expense of configurational entropy. The entropic penalty for spontaneous chain alignment is outweighed by favorable energetic interactions between neighboring segments that are maximized in the aligned state.[12−14]

Previously, we studied segment orientation in PDES elastomers under uniaxial compression using solid-state ^2H NMR.[15] We did not observe any mesophase transition in compression, probably because the network chains could not align in a common direction. At a given compression ratio, the segment orientation (spectral splitting) in compressed, amorphous phase PDES elastomers is greater than that of conventional elastomers such as the more commonly studied PDMS elastomers. We concluded that orientational energetic interactions between neighboring PDES chain segments enhance segment orientation under deformation.

The present work focuses on the structure and orientation within the mesomorphic neck region that forms when amorphous PDES elastomers are subjected to uniaxial extension. We obtain ^2H NMR spectra for a series of stretched PDES networks with well-defined molecular architectures to observe the effects of cross-link density and pendent defects on segment orientation and phase behavior.

We will combine our analysis of the NMR spectra with optical observations and dynamic mechanical analysis to elucidate the orientation process during extension.

Table 1. PDES Network Characteristics

	precursor				
sample	M_n (kg/mol)	M_w/M_n	G_e/RT (mol/m^3)	w(sol) (%)	% CD_2CH_3
Opt-d_2-1	38	1.32	77	0.4	25
Opt-d_2-2	26	1.22	79		25
Opt-d_2-3	20	1.21	77		25
Opt-d_2-4	17	1.17	86	0.5	25
Opt-d_2-5	9.3	1.19	92	1.0	25
Imp-d_2-1	18	1.34	56	3.6	5
Imp-d_2-5	12	1.19	43	6.5	5

Experimental Section

Sample Preparation. Two series of $-CD_2CH_3$-labeled PDES networks were prepared by hydrosilylation end-linking of telechelic precursor chains with tetrafunctional cross-linkers:[3] "imperfect" networks with a high soluble fraction (and therefore many structural defects) and "optimal" networks with minimal soluble fraction (Table 1). The imperfect networks contained 5% $-CD_2CH_3$ ethyl groups and were labeled Imp-d_2-1, Imp-d_2-2, etc. The optimal networks contained 25% $-CD_2CH_3$ ethyl groups and were labeled Opt-d_2-1, Opt-d_2-2, etc. These samples were used previously in our compression studies, and we report here results obtained under uniaxial extension for the networks listed in Table 1. Networks were prepared with $-CD_2CH_3$ groups rather than $-CD_2CD_3$ to simplify the ^2H NMR spectra. The $-CD_2$ deuterons are closely coupled to the orientation of the polymer backbone, so the ^2H NMR spectra reveal the orientation of chain segments. The syntheses of partially deuterated monomer, PDES precursor chains, and networks are described elsewhere.[3,5,15]

The elastomers were molded into strips 1.25 mm thick, 3.75 mm wide, and 30−50 mm long in glass molds made of microscope slides. The resulting samples had smooth surfaces and uniform thickness, a requirement for uniform stretching. Before NMR experiments were conducted, the soluble fractions of the samples were removed by toluene extraction.[16] To check for preexisting orientation in the unstretched elastomers, the samples were viewed between crossed polarizers in a light microscope. No signs of anisotropy were found.

10.1021/ma010408w CCC: $20.00
Published on Web 07/07/2001

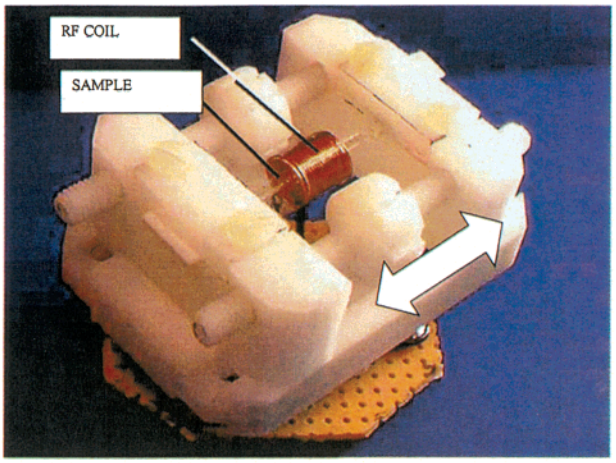

Figure 1. Extension device for ^{2}H NMR measurements.

Optical Microscopy. A Wild Heerbrug M21 polarized light microscope at 40× magnification was used to observe PDES network films that were stretched and held in place by clamping in a stainless steel extension device. The orientation of the stretch axis with respect to the light polarization direction could be controlled by rotating the microscope stage. A Minolta SRT 102 camera with Kodak 800 Max film was used to record photographs through the microscope using a steel eyepiece-projection tube. The samples were observed between crossed polarizers with a 550 nm compensator. The compensator made the birefringence colors easier to differentiate and permitted determination of the "slow" direction in the samples (the direction of highest refractive index). All microscope photos were taken with the stretch direction of the sample oriented at 45° with respect to the "vibration direction" of the polarizer.

Dynamic Mechanical Analysis (DMA). The equilibrium relationship of force vs extension ratio ($\lambda = L/L_0$) for selected PDES elastomers was studied in uniaxial extension with a Perkin-Elmer dynamic mechanical analyzer DMA 7e. Samples were rectangular and measured 10 mm by 3.5 mm by 1.25 mm. For the purposes of this work, force vs extension curves were required at low elongations ($\lambda < 2.2$, amorphous phase only). DMA results at higher extensions showing the effects of the mesophase transition on the mechanical properties of our networks are reported elsewhere.[3]

Shear moduli G_e/RT of the imperfect networks were estimated from DMA extension measurements at a strain of approximately 1% as described previously.[3] Moduli of the optimal networks were estimated from their equilibrium swelling ratios in toluene.[3,5]

Photographic Estimation of Local Extension Ratios. The local extension ratio for the part of the sample inside the NMR coil was determined in each experiment as follows. The surface of the unstretched elastomer was dotted along the long direction using a water-based ink. The ink could not diffuse into the samples. The dots were approximately 0.2 mm diameter and were spaced at intervals of about 0.5 mm. The sample was photographed in the unstretched state. After stretching and waiting for the sample length to stabilize, another photograph was taken. By comparing distances between dots in the photos, it was possible to calculate the local extension ratio.

Stretching Device. A novel extension device made of DuPont delrin (Figure 1) was constructed to fit inside the NMR probe. It is similar to Loo et al.'s device,[17] except that it consists of two sliders, each equipped with a chucking piece that grips an end of the sample. Samples were clamped to the device by compressing them at both ends with set plates and nylon screws, and they could be stretched 10−40 mm by turning two double-ended bolts, which expanded the stretching device along a sliding frame. To induce mesophase formation, samples were stretched to $\lambda > 2$ and cooled to 0 °C in a container over ice for 1 h. After the neck had formed, the samples were allowed to equilibrate at the laboratory temperature (23 °C) for several hours before NMR measurements were commenced. Experiments on stretched PDES samples in the amorphous (nonnecked) state were conducted without any need for cooling or equilibration under the imposed stress.

NMR Spectroscopy. Spectra were obtained on a Bruker CXP200 spectrometer operating at a frequency of 30.721 MHz for deuterium. A Bruker z32vHP probe body with a custom-built probe head and coil was used. The coil chosen to minimize dead volume had length of 8.5 mm, diameter of 7.5 mm, and 19 turns. It was made of 22 gauge copper wire coated with epoxy resin to reduce arcing during the radio-frequency (rf) pulses. The sensitivity of the coil as a function of position along the axis was calibrated using a small deuterated reference sample. The coil was effectively insensitive to deuterated material located more than 4 mm outside the coil. The network samples were oriented such that the extension axis was parallel to the coil axis and perpendicular to the applied magnetic field. The coil covered a uniformly stretched part of the sample (far from the ends). The spectra therefore did not contain any contribution from the clamped ends, which were unevenly deformed.

A simple $(90°)_x$ pulse (typically 6 μs) was found to be adequate for most experiments. The repetition delay between scans was 1 s. For 25% deuterated samples, at least 1800 transients were typically required to achieve a signal:noise ratio of 16 to 1 in the final spectrum. When the samples were stretched to high elongation, more repetitions were required, because the volume of sample in the coil was reduced. For 5% deuterated samples, up to 150 000 scans were accumulated. The spectral broadening due to magnetic field inhomogeneities was estimated to be less than 50 Hz, which was minimal compared to the widths of the PDES methylene deuteron peaks.

The bandwidth and ringdown of a NMR probe circuit can attenuate peaks off-resonance. The attenuation of off-resonance peaks was calibrated by measuring the spectrum of a $-CD_3$-labeled PDMS liquid reference sample at a series of frequencies off-resonance. We observed a 10% attenuation at 10 kHz off-resonance, the extreme position of peaks observed for stretched PDES. The spectra areas reported here are corrected by our calibrations.

Results and Discussion

Optical Microscopy. When amorphous PDES elastomers are stretched to a critical extension ratio (generally $\lambda > 2.0$), a neck region forms. The critical extension ratio depends on the cross-link density and the possible presence of stress concentrators (for example, a dust particle or a small irregularity on the surface). At first, the transition region is irregular (Figure 2a). After a few minutes the neck region stabilizes under the stress, and it assumes a well-defined shape with a distinct transition region (Figure 2b). The neck is highly birefringent, with a very faint crosshatched fibrous structure visible in places. The fibrous texture is oriented along the principal stress axes in the sample, and its alignment is somewhat distorted near the transition zone. The crosshatched structure may be due to organization of mesophase microdomains along the principal stress axes in the elastomers. The fibrous texture is reminiscent of the lamellae observed in the mesophase of un-cross-linked PDES melt of high molecular weight.[11] However, due to the small amount of structure visible in the PDES networks, it is not possible to comment further on the morphology of the neck region.

Amorphous single-phase regions exist on either side of the neck. Although the amorphous material is oriented, it is only weakly birefringent compared to the neck. The amorphous regions are blue, indicating that

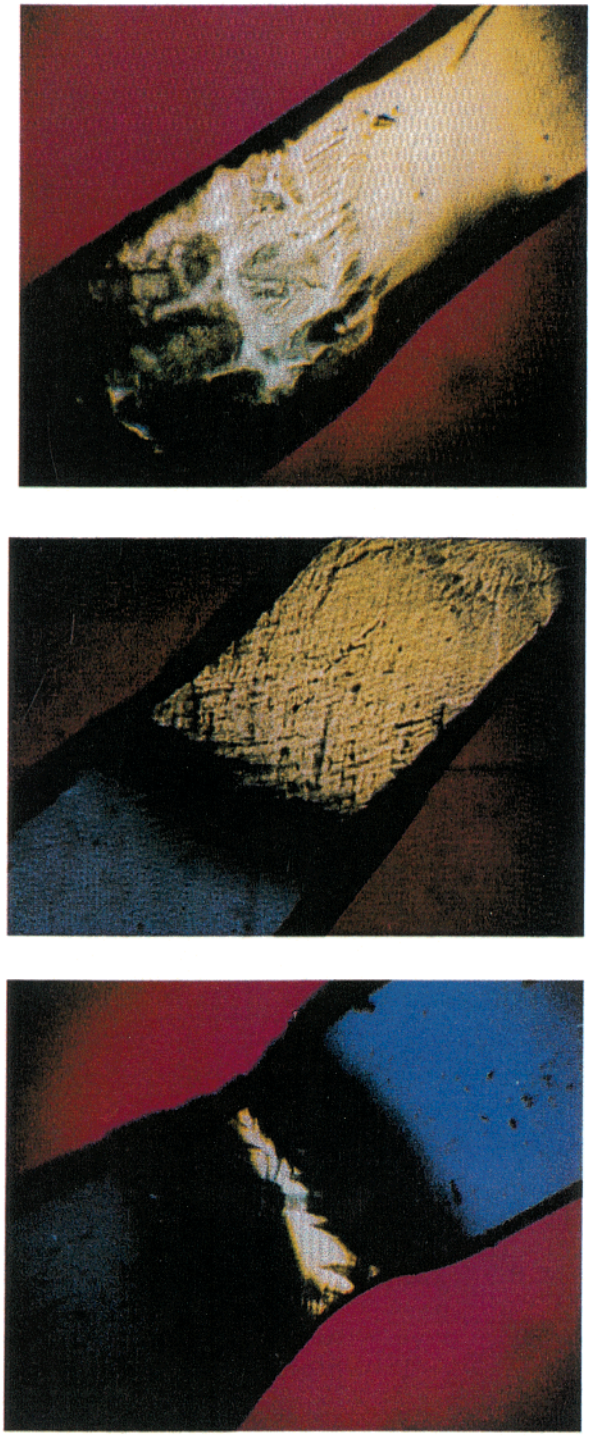

Figure 2. PDES neck region (40×) through crossed polarizers: (a) during transition; (b) after stabilization; (c) when stress is reduced.

the slow direction of the sample is the stretch direction. At the molecular level, this direction usually coincides with the alignment of the chain backbones.[18] When the stress on the sample is released gradually, the amorphous regions consume the neck at the transition zone (Figure 2c).

Photographic Measurement of Local Extension Ratios. An interesting feature of the necking process was noted from the measurements of the local extension ratios of the neck and amorphous regions. Once the neck had formed, further uniaxial stress allowed it to propagate by consuming the amorphous regions. During this

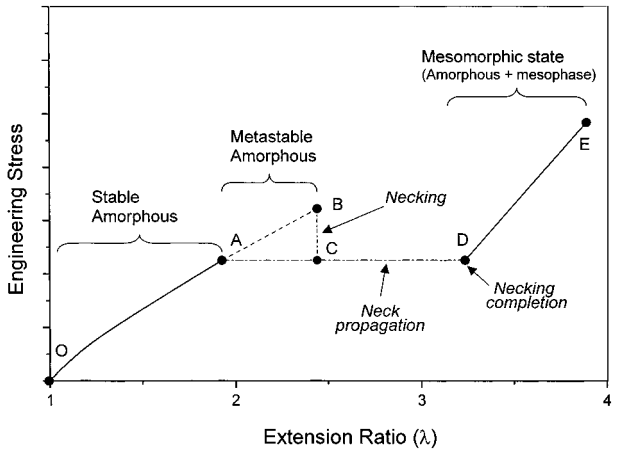

Figure 3. Schematic diagram of engineering stress vs extension ratio for an initially amorphous PDES elastomer.

conversion process, the neck remained at an approximately constant local extension ratio, as did the amorphous regions. These characteristic extension ratios remained constant until the amorphous material was entirely consumed. After the entire sample was necked, further stretching increased the local extension ratio. The separation of the necking process into these two stages was made possible by the uniform thickness of our samples.

The photographic measurements of the local extension ratios were a useful complement to our previously obtained DMA results.[3−5] Figure 3 is a schematic diagram of engineering stress vs extension ratio for an initially amorphous PDES elastomer. When the network is stretched, it lengthens from point "O" to point "A" while remaining in the amorphous phase. Further stretching from point "A" to point "B" in the "metastable" amorphous region causes no apparent phase transition, in part because the mesophase formation is kinetically limited. If the sample is held at "B" long enough, a neck forms and the engineering stress decreases to point "C". If the overall sample length is held constant during the transition, there is an abrupt increase in the local extension ratio in the neck region and a decrease of extension ratio in the amorphous regions. A differential increase in the engineering stress is required to stretch the sample from point "C" to point "D". During this process, amorphous regions are converted to neck, until the entire sample is necked at point "D". Further stretching toward the breaking point "E" requires a significant increase in the engineering stress because the network chains are already highly extended. If the stress is released slowly from a sample initially at point "D", the sample follows the path D → C → A → O without entering the metastable amorphous region. Note that whereas A and D occur at the same strains in every sample, the strain at which the neck forms, point B, varies.

^{2}H NMR Spectra. Spectra were obtained from both stretched amorphous samples and from the neck region of samples that had undergone a mesomorphic transition. Spectra from the intermediate region where the neck was short were not considered because they contained inseparable contributions from different regions of the sample.

1. Amorphous Spectra. At local extension ratios below $\lambda = 2.2$, none of the samples showed a stable mesomorphic state. Spectra of stretched PDES networks in

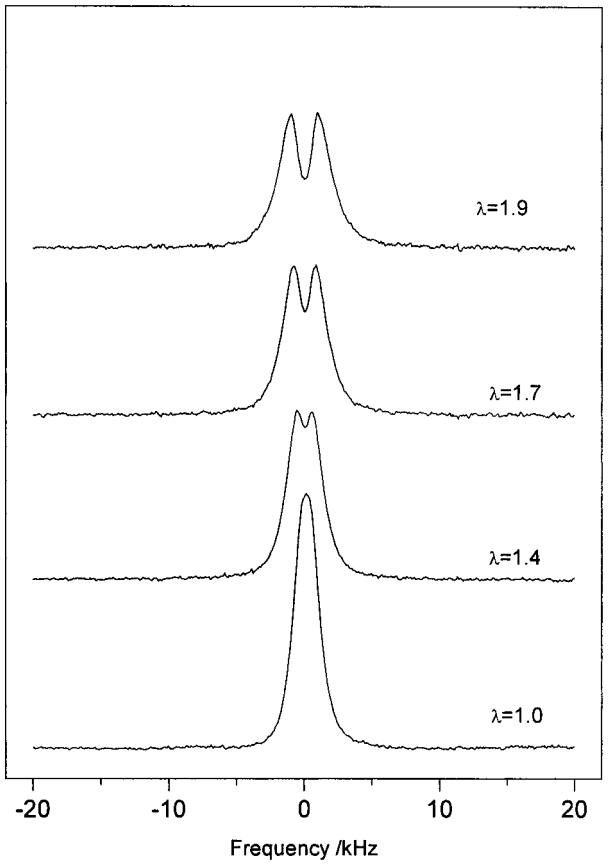

Figure 4. Extension spectra of PDES network Opt-d_2-3 (amorphous state).

the single-phase amorphous state were very similar to those of compressed PDES elastomers.[15] Figure 4 shows spectra for network Opt-d_2-3 as a function of extension ratio. In the unstretched state, a single broad peak of approximately 1 kHz width at half-height was observed. When the sample was stretched, the spectrum split into an overlapping doublet. As the local extension ratio was increased, the splitting increased. Until the neck region forms, the PDES spectra qualitatively resemble those of conventional elastomers.

2. Neck Region Spectra. It was possible to get spectra for the "pure" neck region when the neck was at least several millimeters longer than the coil. Neck region spectra for sample Opt-d_2-3 at various local extension ratios are shown in Figure 5. Two characteristic mesophase peaks appeared with a splitting of 19.1 kHz and a typical width at half-height of about 1 kHz. These peaks were clearly separated from the amorphous peaks in the central portions of the spectra, confirming that the neck region contains two distinct phases. As the extension ratio increased, the mesophase peaks grew at the expense of the amorphous peaks, indicating conversion of amorphous material to mesophase.

Because the splitting and shape (but not the fractional area) of the mesophase peaks were independent of the extension ratio, we concluded that the structure and orientation within the mesophase lattice remained constant, independent of extension ratio. The relatively sharp, axially symmetric mesophase peaks indicated that the chain backbones are aligned in a common direction, which was determined by optical microscopy to be the extension axis.

The spectral splitting from the mesophase of our samples is 19 kHz (inset of Figure 6). The splitting

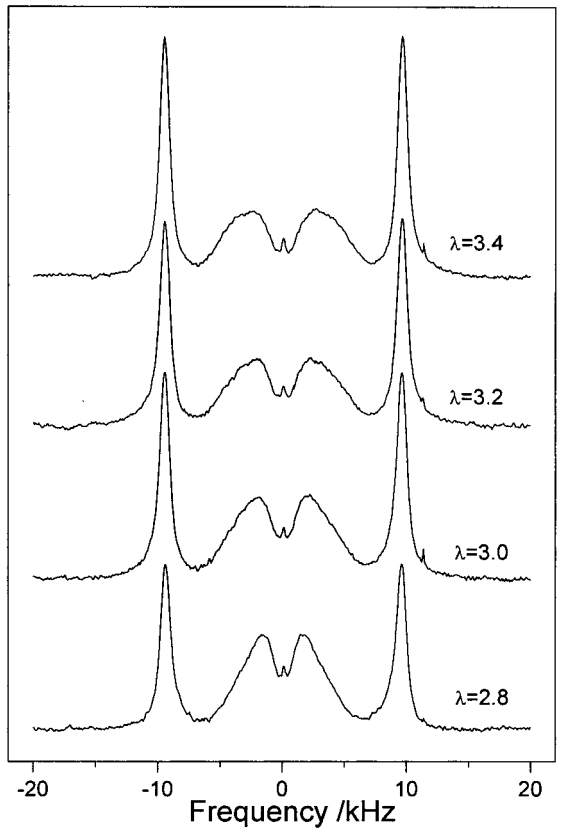

Figure 5. Extension spectra of PDES network Opt-d_2-3 (biphasic necked state).

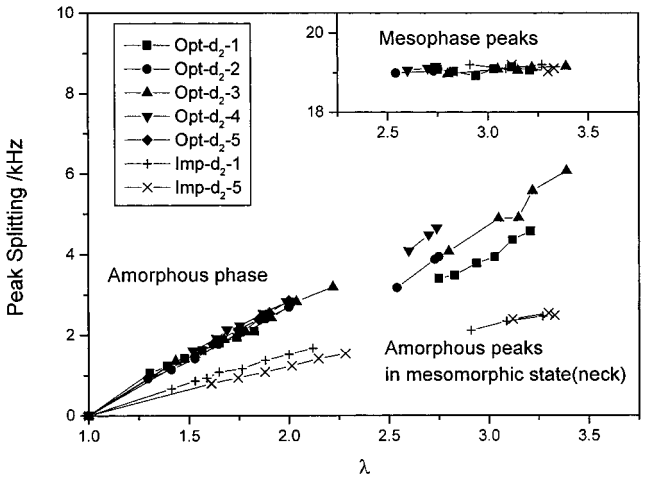

Figure 6. Amorphous peak splitting vs λ for all samples.

between the maxima from the powder pattern spectra of linear (un-cross-linked) PDES mesophase was also reported elsewhere to be 19 kHz.[19] The linear PDES studied in ref 19 contained mesophase microdomains with random orientations leading to a powder pattern, whereas the mesophase in our networks contained chains with a common orientation.

In contrast to the mesophase peaks, the amorphous peaks changed with extension ratio. The amorphous peak splitting increased, and the component peaks broadened asymmetrically about their maxima. The broadening of the amorphous peaks was similar to that observed in compression experiments at higher deformations ($\lambda < 0.8$).

The qualitative features of the spectra suggest the following picture of the PDES network microstructure

during the stretching process. Once the neck region forms, the single-phase amorphous regions adjacent to the neck are consumed by the neck. When the sample is completely necked, further stretching converts amorphous material within the neck to mesophase. In addition, amorphous material within the neck orients further without undergoing a phase transition. However, stress causes no further increase in the orientation of the mesophase itself. The spontaneous molecular shape change accompanying the amorphous-to-mesophase transition is the primary mechanism for lengthening of the sample.

Calculation of Spectral Splittings. *1. Single-Phase Amorphous Samples.* For nonnecked samples, the line shapes could be fitted reasonably to the sum of two identical Lorentzian functions. The splitting was taken as the distance between the centers of the component peaks. In our prior PDES network compression experiments,[15] spectra at low deformation ($\lambda > 0.8$) could also be fitted reasonably to a single pair of Lorentzian functions, but the line shape became noticeably distorted as deformation increased. The observed line shapes were inconsistent with a recently published analytical expression for the spectra of a strained network.[20]

2. Amorphous Material within the Biphasic Neck Region. In this case, the amorphous component peaks showed asymmetric broadening about their maxima, so they could not be reliably fitted to a single pair of Lorentzian functions. The same procedure we used to decompose PDES network compression spectra[15] was therefore employed. Spectra were assumed to be the sum of two pairs of Lorentzian functions having the same center. The center, peak widths, and splittings of the individual pairs were optimized to give the best overall fit. Typically, the pair with the larger splitting had broader components. The splitting was defined as the separation between the maxima of the fitted doublet components. The asymmetry of the line shapes of amorphous regions could be caused by the fact that, unlike the mesophase regions, the amorphous regions consist of molecules whose degree of orientation depends on their proximity to the aligned mesophase domains. In some spectra (as in Figure 5), a small third peak was observed near the center. This peak usually had a fractional area of less than 1% of the total spectrum and often had an irregular or inconsistent shape. Although we neglect this peak in the data analysis, it was included in the fitting algorithm as a single Lorentzian peak.

Dependence of the Quadrupolar Splittings on Extension Ratio. The frequency splittings, $\Delta\nu$, for all the amorphous structures are plotted in Figure 6 as a function of local extension ratio, λ. In the necked state, the reported splittings are for the amorphous material within the biphasic neck. The inset in Figure 6 shows the (constant) splitting of the mesophase peaks as a function of local extension ratio.

For the splitting data in the nonnecked samples, a mathematical expression for the dependence of $\Delta\nu$ on extension ratio λ was sought. The quadrupolar peak splitting $\Delta\nu$ reflects segment orientation in subtle ways and can be shown[21,22] to be proportional to the segment order parameter **S**,

$$\Delta\nu \propto \mathbf{S} \propto \langle P_2(\cos\theta)\rangle \qquad (1)$$

where θ is the angle between the tangent vector of a given segment and the applied magnetic field. P_2 is the second Legendre polynomial, and the brackets are an average over the distribution of segment orientation in the sample. By assuming affine deformation and Gaussian chain statistics, Kuhn and Grun[23] proposed that $\mathbf{S} \propto (\lambda^2 - \lambda^{-1})$. Experimentally, $\Delta\nu$ has indeed been found to be directly proportional to $(\lambda^2 - \lambda^{-1})$ for conventional elastomers,[21,24−28] including PDMS. On the other hand, the splitting of PDES networks under compression exhibits a nonlinear behavior as a function of $(\lambda^2 - \lambda^{-1})$.[5,15] Such a nonlinearity is also observed for PDES networks under extension.

The nonlinear relation between $\Delta\nu$ and $(\lambda^2 - \lambda^{-1})$ may be due to an orientation-dependent energetic interaction between neighboring PDES chain segments. Previously, we analyzed PDES network compression data[15] in terms of a model of Brereton and Ries.[22] This model predicts spectral splittings based on excluded-volume interactions between segments. The experimental splittings for compressed PDES networks were substantially higher than the predictions based on excluded-volume arguments. Thus, we proposed that energetic couplings between PDES chain segments enhance orientation when the networks are deformed. The proposed energetic interactions are consistent with the decrease of internal energy in PDES elastomers that accompanies mesophase formation during stretching.[1,2,14,29−31]

The proportionality between $\Delta\nu$ and $(\lambda^2 - \lambda^{-1})$ for conventional elastomers was derived[23] assuming Gaussian chain statistics and affine deformation. Given the tendency of PDES chains to align spontaneously, neither of these assumptions may be strictly correct, even at low deformations in the amorphous state. Thus, plotting $\Delta\nu$ vs $(\lambda^2 - \lambda^{-1})$ may not be physically meaningful.

An alternate way to examine the spectral data is to plot the splittings $\Delta\nu$ vs the stress in the sample, σ. The need for a model of chain statistics and the assumption of affine deformation are eliminated, because only experimental parameters are plotted. An experimental measurement of the engineering stress σ^* vs λ was obtained by DMA for three networks: Opt-d_2-2, Opt-d_2-3, and Imp-d_2-5.

The σ^* vs λ curves could not be modeled by a network of chains with Hookean tension (Gaussian chain statistics) or by the inverse Langevin expression of tension. The results were therefore fitted to the empirical Mooney−Rivlin equation:[32]

$$\sigma^* = (C_1 + C_2/\lambda)(\lambda^2 - \lambda^{-1}) \qquad (2)$$

Table 2 lists the calculated Mooney−Rivlin parameters for the three samples.

Table 2. Mooney−Rivlin Constants (Best Fits) for Selected PDES Networks

sample	C_1	C_2
Opt-d_2-2	37.6	77.3
Opt-d_2-3	43.1	73.0
Imp-d_2-5	32.6	33.2

Because most of our samples were broken during NMR measurement, the limited DMA data in Table 2 were used to estimate the actual stress in the other networks. Imp-d_2-5 was taken as a model for Imp-d_2-1, and the average of samples Opt-d_2-2 and Opt-d_2-3 was taken as a model for the other optimal networks. (A simple correction for modulus was applied to simulate DMA data for the other samples.)

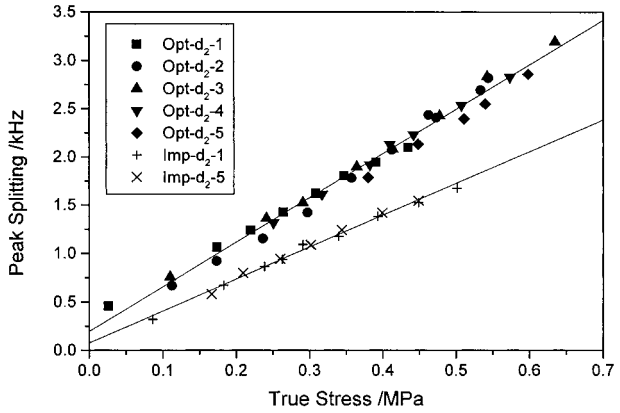

Figure 7. Amorphous peak splitting vs true stress for nonnecked samples.

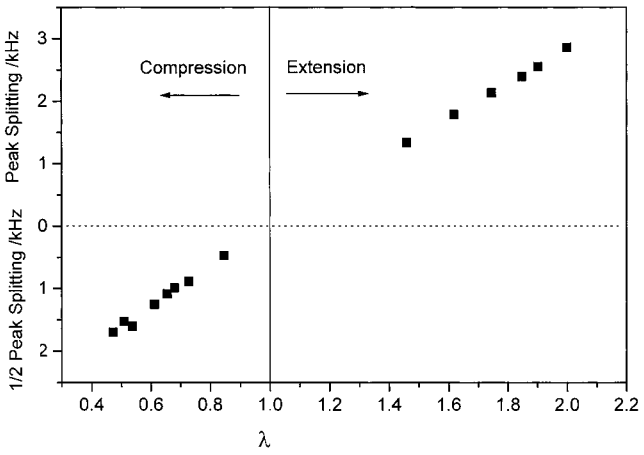

Figure 8. Comparison of spectral splittings in extension and compression for network Opt-d_2-5.

Values of the engineering stress σ^* were converted to values of true stress σ by assuming constant volume during stretching and using the relationship $\sigma = \lambda\sigma^*$. When NMR splittings were plotted vs true stress, a near linear relationship was found (Figure 7). Assuming $\Delta\nu \propto \mathbf{S}$, the order parameter **S** is linear with the true stress. Note the nonzero intercepts in Figure 7, however. The intercept for the imperfect samples was closer to zero than for the optimal samples. These results share a common feature with the compression data reported elswhere.[15] The optimal networks exhibit an abrupt increase in segment orientation at low deformations in both cases. This increase is less pronounced for the imperfect samples. Here, as in the compression experiments, the segment orientation may be enhanced by energetic interactions between chains. The chain segments may locally align with each other in the nondeformed state, even though the overall orientation is isotropic. When slight deformation is applied, the local orientation shifts to the direction of stress, and an increased spectral splitting is observed. The broad line widths of the PDES spectra (an order of magnitude larger than for PDMS) indicate incomplete (anisotropic) motional averaging of segment orientation, supporting the idea of orientational association of neighboring segments.

A combined plot of the extension and compression spectral splittings data vs extension ratio showed a continuous trend. Figure 8 shows $\Delta\nu$ vs λ for extension and $^1/_2\Delta\nu$ vs λ for compression[15] for the network Opt-d_2-5. The factor of $^1/_2$ difference arose in the averaging

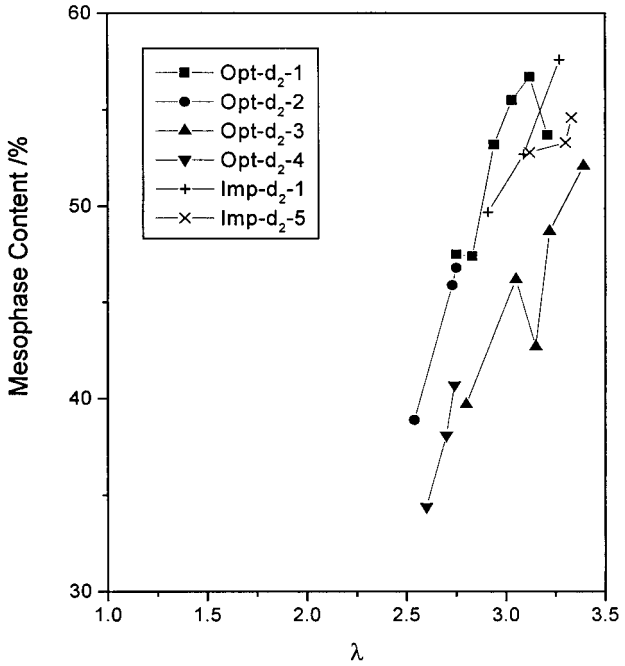

Figure 9. Neck region mesophase content vs extension ratio.

of $\langle P_2(\cos\theta)\rangle$ in eq 1 depending on whether the deformation axis was perpendicular to the applied magnetic field (extension) or parallel (compression). For this particular sample, the data of peak splitting vs true stress (lozenges) shown in Figure 7 as well as the data in Figure 8 appear to go continuously through the origin, and the nonlinearity of the data discussed above appears to be negligible.

Dependence of Neck Mesophase Content on Network Structure. Because the mesophase and amorphous peaks were clearly separated, the ^{2}H NMR spectral areas allowed for unambiguous calculation of the mesophase fraction in the neck region. The percentage mesophase in the samples is shown as a function of extension ratio in Figure 9. Only a small range of local extension ratios could be studied for the neck region because attempts at higher elongation broke the samples. The percentage mesophase as the neck region is stretched clearly increases for all the samples. The mesophase content of the samples ranged from 35% to about 60%, depending on elongation.

Despite the limited data in Figure 9, a trend is visible: the samples with the highest degrees of chemical cross-linking have the lowest mesophase content. This observation is consistent with previous results from thermodynamic analysis.[1] Samples Opt-d_2-1 and Opt-d_2-2 incorporated the least amount of cross-linker due to the high M_n of their precursors. Samples Opt-d_2-3 and Opt-d_2-4 have lower precursor M_n, higher chemical cross-link density, and lower mesophase content. The imperfect networks have low precursor M_n but are expected to have many divalent cross-linkers (due to incomplete reactions), increasing the actual molecular weight between effective chemical cross-links. These networks will also have numerous pendent chains that probably participate freely in the mesophase formation.

Interestingly, there was no correlation between the network modulus and the percentage mesophase because of the opposing effects of cross-link density and network imperfections. For example, the imperfect networks have the lowest moduli by far but lie in the

middle of the range of mesophase content of the optimal networks with much higher moduli. The data of Figure 9 suggest that the nonlinear cross-link sites cannot be forced into a mesomorphic lattice, which disrupts the crystallinity. It is likely that cross-link sites are surrounded by regions of amorphous material. On the other hand, network defects (linear cross-link sites and pendent chains) enhance the extent of crystallinity in a stretched sample.

Conclusion

The combined information from optical microscopy, DMA, and ^{2}H NMR spectroscopy provide a clear picture of the orientation process in PDES networks under uniaxial extension. The networks are initially amorphous, until a certain elongation where a spontaneous alignment takes place, resulting in the neck region. The neck contains two distinct phases: an ordered mesophase and an amorphous phase. Chain axes of the mesophase are oriented in the direction of extension. The neck is in equilibrium with single-phase amorphous regions on either side. As the overall extension ratio of the sample is increased, the neck region grows at the expense of the amorphous regions. During this process, the local extension ratios of both the neck and the single-phase regions remain constant. The sample elongates primarily by conversion of single-phase amorphous material to mesomorphic neck. Once the entire sample is necked, the neck extension ratio increases by conversion of amorphous material within the neck to mesophase and by further orientation of amorphous material. Once the sample reaches a limiting extension, it breaks.

Acknowledgment. H. T. thanks Oji Paper Co., Ltd., for supporting his studies at Cornell University. We gratefully acknowledge the support of the National Science Foundation Polymers Program under Grant DMR-0078863.

References and Notes

(1) Godovsky, Y. K. *Angew. Makromol. Chem.* **1992**, *202/203*, 187.
(2) Papkov, V. S.; Godovsky, Yu, K.; Svistunov, V. S.; Zhdanov, A. A. *Polym. Sci. USSR* **1989**, *31*, 1729.
(3) Hedden, R. C.; Saxena, H.; Cohen, C. *Macromolecules* **2000**, *33*, 8676.
(4) Saxena, H. M.S. Thesis, Cornell University, 2000.
(5) Hedden, R. C. Ph.D. Dissertation, Cornell University, 2000.
(6) Finkelmann, H.; Wermter, H. *Proc. Am. Chem. Soc., Div. Polym. Mater.: Sci. Eng.* **2000**, *82*, 319.
(7) Finkelmann, H.; Rock, H. J.; Rehage, G. *Makromol. Chem., Rapid Commun.* **1981**, *2*, 317.
(8) Yang, Y.; Kloczkowski, A.; Mark, J. E.; Erman, B.; Bahar, I. *Macromolecules* **1995**, *28*, 4927.
(9) Kirste, R. G.; Ohm, H. G. *Makromol. Chem., Rapid Commun.* **1985**, *6*, 179.
(10) D'allest, J. F.; Sixou, P.; Blumstein, R. B.; Teixeira, J.; Noirez, L. *Mol. Cryst. Liq. Cryst.* **1988**, *155*, 581.
(11) Molenberg, A.; Möller, M. *Macromolecules* **1997**, *30*, 8332.
(12) Shibanov, Yu. D. *Polym. Sci. U.S.S.R.* **1989**, *31*, 2653.
(13) Mark, J. E.; Chiu, D. S.; Su, T.-K. *Polymer* **1978**, *19*, 407.
(14) Godovsky, Yu. K.; Volegova, I. A.; Valetskaya, L. A.; Rebrov, A. V.; Novitskaya, L. A.; Rotenburg, S. I. *Polym. Sci. U.S.S.R.* **1988**, *30*, 329.
(15) Hedden, R. C.; McCaskey, E.; Cohen, C.; Duncan, T. M. *Macromolecules* **2001**, *34*, 3285.
(16) Patel, S. K.; Malone, S.; Cohen, C.; Gillmor, J. R.; Colby, R. H. *Macromolecules* **1992**, *25*, 5241.
(17) Loo, L. S.; Cohen, R. E.; Gleason, K. K. *Macromolecules* **1999**, *32*, 4359.
(18) Hemsley, D. A. *Appied Polymer Light Microscopy*; Elsevier Applied Science: New York, 1989.
(19) Litvinov, V. M.; Macho, V.; Spiess, H. W. *Acta Polym.* **1997**, *48*, 471.
(20) Ries, M. E.; Brereton, M. G.; Klein, P. G.; Ward, I. M.; Ekanayake, P.; Menge, H.; Schneider, H. *Macromolecules* **1999**, *32*, 4961.
(21) Gronski, W.; Stadler, R.; Jacobi, M. *Macromolecules* **1984**, *17*, 741.
(22) Brereton, M. G.; Ries, M. E. *Macromolecules* **1996**, *29*, 2644.
(23) Kuhn, W.; Grun, F. *Kolloid Z.* **1942**, *101*, 248.
(24) Deloche, B.; Beltzung, M.; Herz, J. *J. Phys., Lett.* **1982**, *43*, 763.
(25) Toriumi, H.; Deloche, B.; Beltzung, M.; Herz, J.; Samulski, E. *Macromolecules* **1986**, *19*, 2884.
(26) Sotta, P.; Deloche, B.; Herz, J.; Lapp, A.; Durand, D.; Rabadeux, J. C. *Macromolecules* **1987**, *20*, 2769.
(27) Dubault, A.; Deloche, B.; Herz, J. *Macromolecules* **1987**, *20*, 2096.
(28) Jacobi, M.; Abetz, V.; Stadler, R.; Gronski, W. *Polymer* **1996**, *37*, 1669.
(29) Papkov, V. S.; Kvachev, Yu. P. *Prog. Colloid Polym. Sci.* **1989**, *80*, 321.
(30) Godovsky, Yu. K.; Volegova, I. A.; Rebrov, A. V. *Polym. Sci. U.S.S.R.* **1990**, *32*, 726.
(31) Godovsky, Yu. K.; Valetskaya, L. A.; Papkov, V. S. *Makromol. Chem., Macromol. Symp.* **1991**, *48/49*, 433.
(32) Mooney, M. *J. Appl. Phys.*, **1948,** *19*, 434. Rivlin, R. S. *Philos. Trans. R. Soc. London, Ser. A* **1948**, *241*, 379.

MA010408W